AN EXPERIMENTAL RESEARCH ON A CW CO_2 LASER THRUSTER

Kazuhiro Toyoda*, Kimiya Komurasaki † and Yoshihiro Arakawa ‡
University of Tokyo
Hongo, Bunkyo-ku, 113-8656, Tokyo, JAPAN

Abstract

This paper reports results of fundamental experiments on a continuous-wave CO_2 laser thruster. The Laser-Sustained Plasma (LSP) was maintained under pressures ranging from 2 to 7 atm with laser power level of more than 300 watts. The location of LSP was controlled by adjusting laser power and focus position . Thruster performance was then evaluated by measuring thrust using a simple thrust stand equipped with a load-cell sensor. Finally, energy balance in the thruster was understood by measuring heat loss and transparent laser loss.

Introduction

Laser propulsion has been put forth as one of the suitable propulsion concepts for use in space or the atmosphere. Laser propulsion has an acceleration mechanism in which a propellant gas is heated by a laser-sustained plasma (LSP) , which absorbs the high power laser beam from a remote site and is maintained in the thruster, and the gas enthalpy is recovered as thrust by a nozzle. Its payload fraction is expected to become higher than other propulsion systems because space vehicles need not load power sources [1]. Especially as the launcher from the ground, laser propulsion has the advantage of using the air flowing around a rocket as a propellant.

Either a continuous-wave (CW) laser or a pulse laser can be applied in laser propulsion. In this study, a CW laser is employed for laser propulsion experiments. Keefer et al. [2] investigated the fundamental behavior of the LSP and developed a numerical code for the LSP for the purpose of designing a laser thruster. Mazumder et al. [3] performed experiments similar to those of Keefer, but were able to maintain the LSP with higher power levels (~10kW)[4]. However, there have been a limited number of experimental studies on laser propulsion and, in these studies, only thrust has been measured to evaluate thruster performance. There are very few experiments investigating energy transfer from LSP to kinetic energy of a working fluid.

In the present study, laser thrusters were manufactured for fundamental experiments. The LSP was produced even in low power conditions and the shape and positions of the LSP were observed using a CCD camera. In addition, heat loss to the walls and laser power loss passing through the throat were measured and energy transfer processes from the LSP to the propellant gas were investigated.

Concept of Laser Propulsion

The model of laser propulsion is shown in Fig. 1. A laser beam is focused into a plasma production chamber through a set of condensing lens and window. Once a plasma is produced near a focal point, the plasma efficiently absorbs a beamed laser power through inverse bremsstrahlung radiation. The high temperature LSP (about 10,000 ~ 20,000 K) heats a propellant gas, and

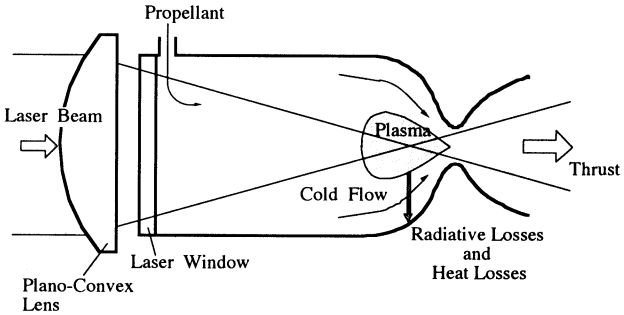

Fig. 1 Sketch of the laser propulsion concept.

*Graduate Student, Department of Aeronautics and Astronautics, University of Tokyo.

† Assistant Professor, Department of Aeronautics and Astronautics, University of Tokyo, Member AIAA/ JSASS.

‡ Professor, Department of Aeronautics and Astronautics, University of Tokyo, Member AIAA/ JSASS.

then the thermal energy of the gas is converted into the kinetic energy through a convergent-divergent nozzle. The convective heat transfer to the chamber wall is usually small because the core of LSP does not attach directly to the wall, having cold flow surrounding the LSP. On the other hand, the radiative loss from the LSP increases with an increase in temperature of LSP. Accordingly, the performance of laser propulsion depends on the energy balance in the energy transfer processes.

Experimental Apparatus

Figures 2 (a) and (b) show the cross section of both the laser thruster and the thruster with an observation window. Both thrusters consist of a laser window, a plasma production chamber and a nozzle. In the case of the thruster with an observation window, a plate with a orifice was installed instead of a nozzle. The laser window is a zinc selenide (ZnSe) disk with anti-reflection coating and can transmit a laser beam of 10.6 μm wavelength efficiently. It withstands up to 10 atm. This window was sealed by silicone sheets. The chamber and window were cooled by means of regenerative cooling of propellant gases. Argon and nitrogen were used as propellants, with flow rates up to 50 l/min (1.48 g/sec in argon, 1.04 g/sec in nitrogen).

The thruster has a sub-chamber upstream from the throat. The diameters of the sub-chamber entrance, the straight section, and the throat are 3 mm, 6 mm and 1 mm, respectively. The throat is made of tungsten in order to withstand high heat flux from the laser beam and plasma radiation. The nozzle was water-cooled to

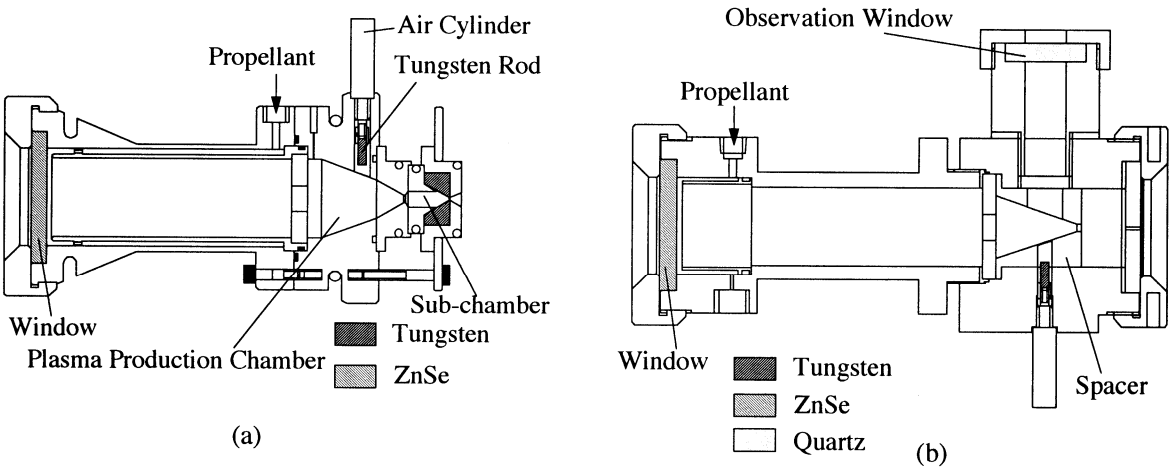

Fig. 2 Cross section of both thrusters.
(a) laser thruster, (b) thruster with observation window

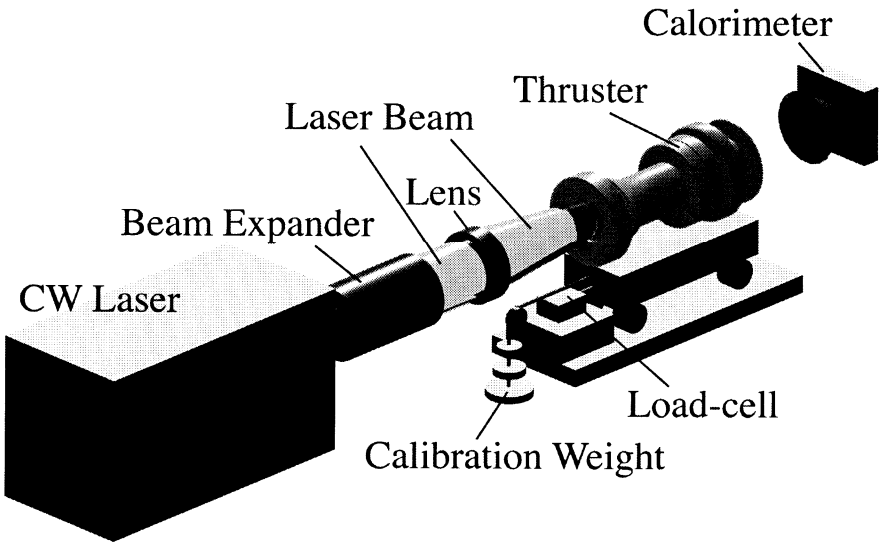

Fig. 3 Schematic of experimental apparatus.

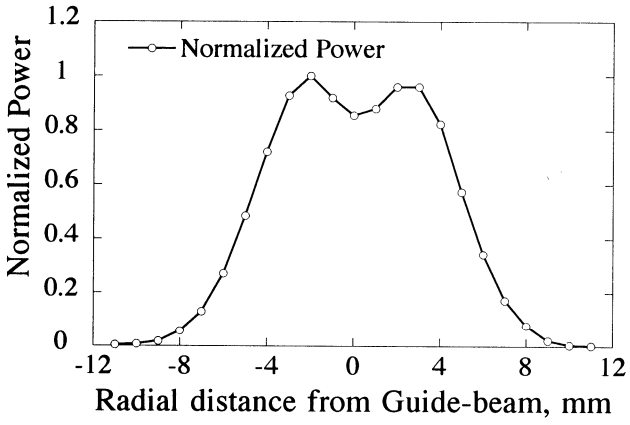

Fig. 4 Energy distribution across beam annulus at 700 W.

measure the heat loss to the wall.

In the case of the thruster with an observation window, this part was placed on the plasma production chamber, enabling visualization of the LSP with a CCD camera through the window. A division disk was installed to prevent the laser beam from reflecting on the walls. The orifice was 1 mm in diameter and the propellant pressure was about 6 atm at 1.5 g/sec argon gas.

To ignite a plasma, a tungsten rod was used as the source of electron emission. This tungsten rod was inserted into the focal point and then pulled back after a plasma was produced.

Figure 3 shows a schematic of the experimental apparatus. The thruster was mounted on two parallel rails, reducing friction in the thrust direction. The thrust was measured by a load-cell censor, and an array of weights was used for thrust calibration. As a result, the drift from zero point was quite small and the reproducibility of thrust measurement was confirmed.

The heat loss to the wall was obtained by measuring the increase in cooling water temperature measured with thermocouples. The laser energy passing through the throat was measured with a calorimeter.

In these experiments, a 2 kW (CW) CO_2 laser (Panasonic YB-L200B7T4) was utilized. The laser power was varied during operation. The energy distribution across the beam annulus is shown in Fig. 4. The beam diameter was magnified by 2.2 using a ZnSe beam expander, and the magnified beam was focused into the thruster through a ZnSe plano-convex lens of 250 mm focal length. This lens was mounted on a one-axis stage movable in the laser beam direction. The LSP location changed as the location of the focal point was varied. Both the beam expander and the condensing lens were cooled with circulating oil.

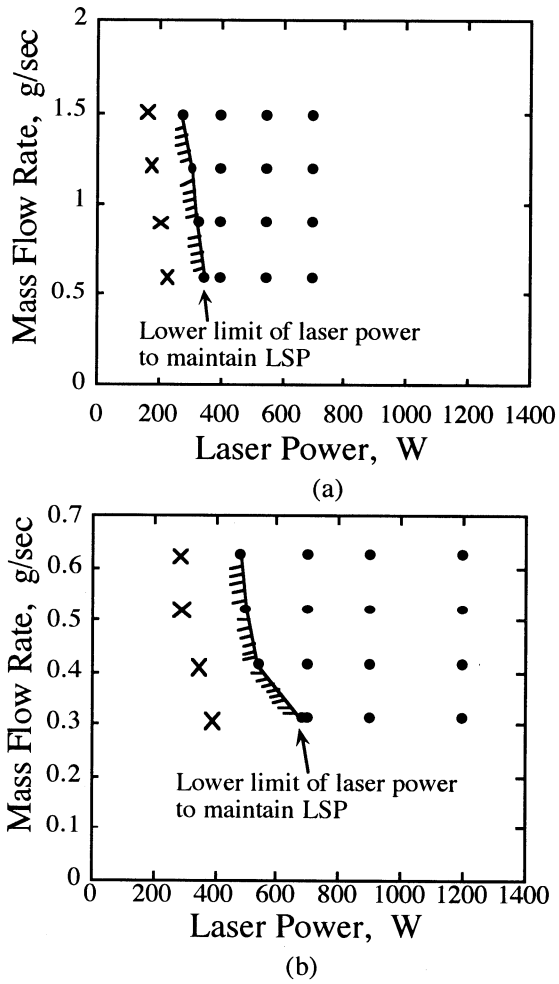

Fig. 5 Operating conditions for maintaining a stable LSP. (a) Ar, (b) N_2

Experimental Results

Production and Sustainment of Plasma

In order to achieve plasma ignition, the tungsten rod had to be heated up with laser power of more than 700 W for several seconds. Figures 5 (a) and (b) show the operating conditions of maintaining a stable LSP in the case of argon and nitrogen respectively. The lower limit of the laser power can be reduced with increasing mass flow rate. However, in the case of nitrogen, the lower limit was higher than that in the case of argon. This is because argon is more easily ionized and can absorb the laser beam power more efficiently.

Behavior of LSP

The thruster with the observation window was used to view the shape and position of LSP in the chamber. The image of LSP taken by a CCD camera through a quartz window is shown in Fig. 6. A band pass filter and a ND filter were used. Once the plasma was ignited, the LSP moved upstream to the region where it could be observed. We were able to move the LSP back to the

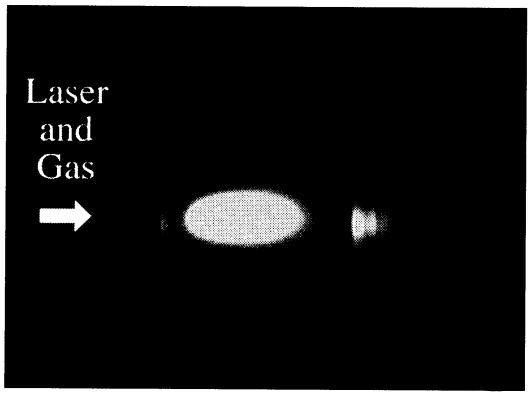

Fig. 6 Image of LSP taken by CCD camera. Propellant gas is argon.

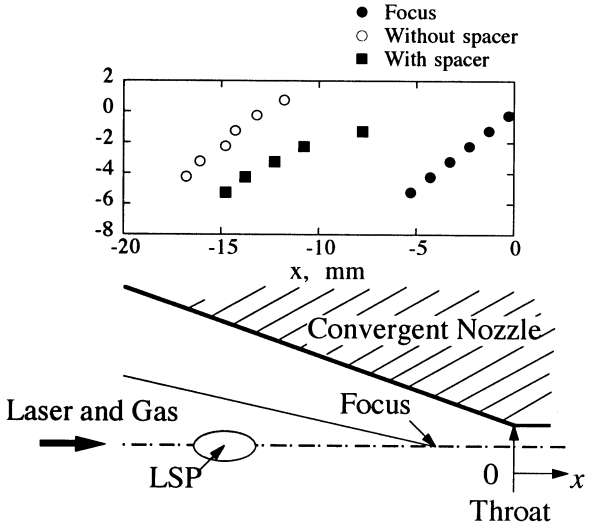

Fig. 7 Relation between focus position and plasma's position.

observable region by means of moving the focus position to take its image. In the picture, the laser and gas were supplied from the left hand side.

Figure 7 shows the relation between the focus position and the LSP position. The movement of the LSP position was proportional to that of the focus position without the spacer. On the other hand, with the spacer, the movement of the LSP was larger than that of the focus position. This means that the LSP moved downstream as it moved into the smaller sectional area in the spacer.

The gas pressure became higher when the LSP moved closer to the throat at a constant mass flow rate, resulting in higher thrust and better performance.

Thrust Measurement

For the thrust measurement, argon was used as the propellant. Figure 8 shows the time sequence of the change in thrust as the focal point moves from the

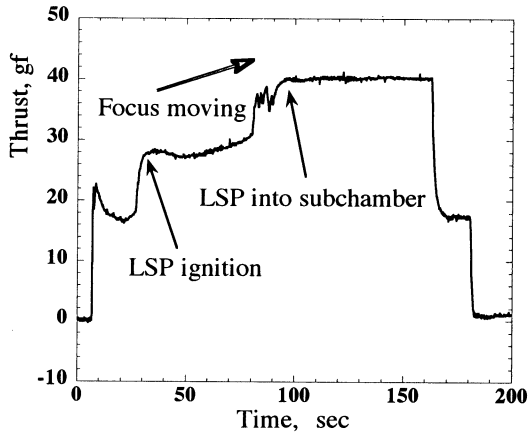

Fig. 8 Time sequence of thrust at 700 W and 0.593 g/sec.

production chamber to the subchamber. The gas pressure increased gradually when the LSP approached the entrance of the sub-chamber, and increased remarkably when the LSP entered the sub-chamber.

Figure 9 shows the relation between thrust and gas pressure. The thrust was proportional to the pressure for any mass flow rate and laser power. Therefore, it seems that the ideal aerodynamic acceleration through the Laval nozzle is valid for this thruster. Thrust is usually evaluated by the following equations [5].

$$F = C_F A_t p_c \tag{1}$$

$$C_F = \sqrt{\frac{2k^2}{k-1}\left(\frac{2}{k+1}\right)^{(k+1)/(k-1)}\left[1-\left(\frac{p_e}{p_c}\right)^{(k-1)/k}\right]} \tag{2}$$

where F is thrust, C_F thrust coefficient, A_t cross-sectional area of the throat, p_c chamber pressure, p_e nozzle exit pressure, and k specific heat ratio. Figure 10 shows the thrust coefficient obtained from the measured thrust and pressure. In this figure, the solid line represents the theoretical value calculated from Eq. (2). In this experiment, the measured C_F was close to 1.0 at around 4 atm and agreed well with the theoretical value. If a high pressure ratio P_c/P_e were realized, thruster performance would be enhanced.

From the choking condition at the throat, the mass flow rate is defined as,

$$\dot{m} = p_c A_t \frac{k\sqrt{\left(\frac{2}{k+1}\right)^{k+1/k-1}}}{\sqrt{kRT}} \tag{3}$$

The nozzle conversion efficiency is defined using Eqs. (2) and (3):

$$\eta_N = \frac{\frac{F^2}{2\dot{m}}}{\dot{m}C_pT} = 1 - \left(\frac{p_e}{p_c}\right)^{\frac{k-1}{k}} \quad (4)$$

η_N is a function of only the pressure ratio p_c/p_e.

The stagnation gas temperature in the chamber can be estimated using Eq. (3) as,

$$T_c = \frac{p_c^2 A_t^2 k\left(\frac{2}{k+1}\right)^{k+1/k-1}}{\dot{m}^2 R} \quad (5)$$

Figure 11 shows the gas temperature calculated from the measured pressure and mass flow rate. The gas temperature rose with increasing laser power and the maximum value was about 1200 K.

Energy Losses Measurement

The heat loss flux to the surrounding walls can be estimated by the product of the flow rate of cooling water

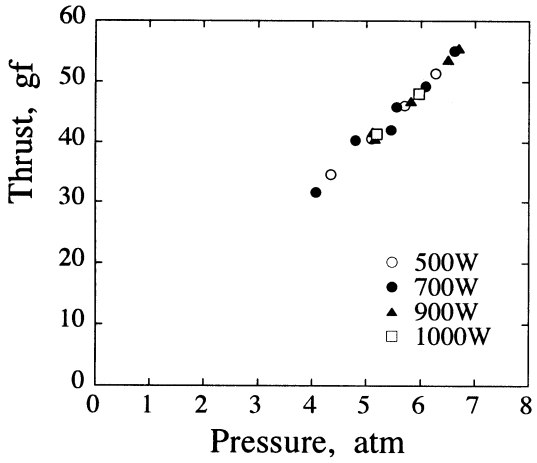

Fig. 9 Relation between thrust and static pressure.

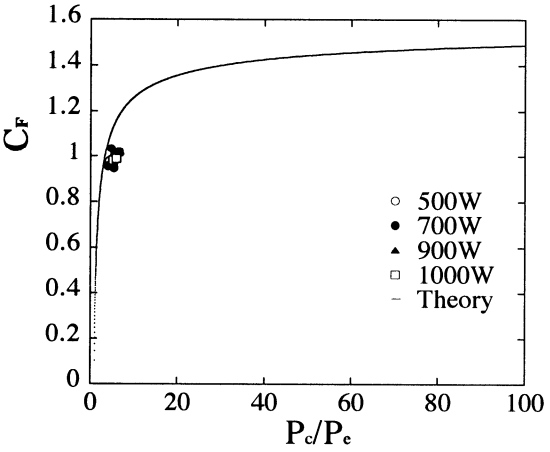

Fig. 10 Thrust coefficient calculated using measured thrust and pressure as a function of pressure ratio.

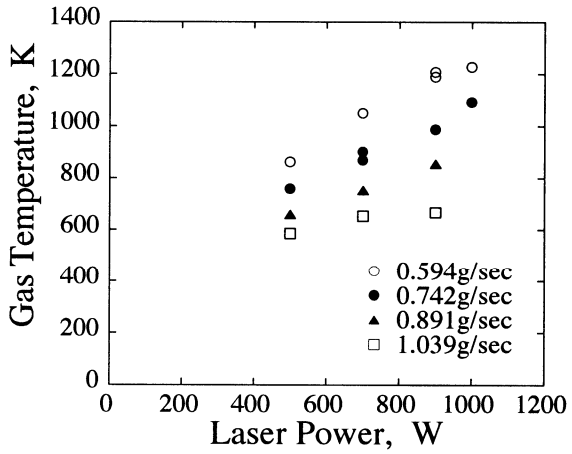

Fig. 11 Gas temperature as a function of incident laser power.

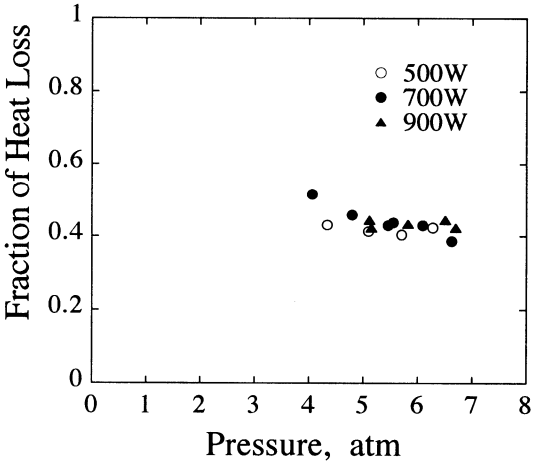

Fig. 12 Relation between fraction of heat loss and pressure.

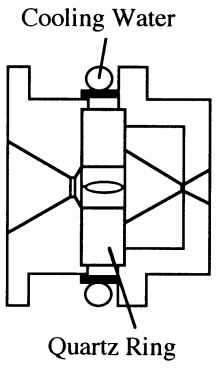

Fig. 13 Nozzle configuration for radiation measurements.

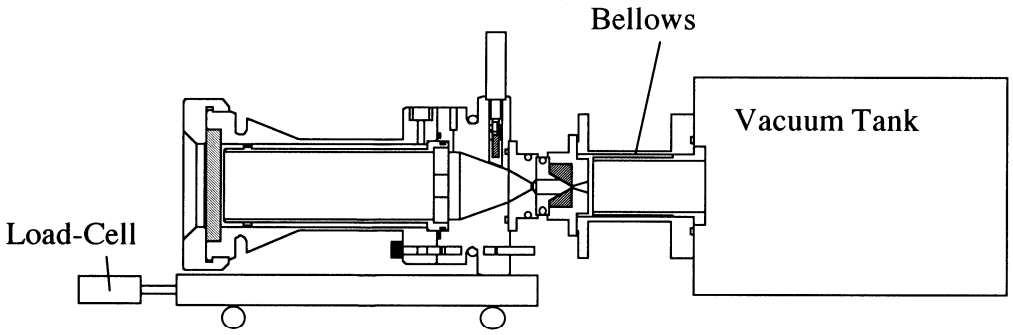

Fig. 14 Thrust measurement system with vacuum tank.

Table 1 Increase in energy conversion efficiency with rising pressure ratio

Plenum pressure (atm)	5	5
Pressure ratio	5	300
Thrust increase (gf)	23	38
Cold thrust (gf)	16	(24)
Energy conversion efficiency	0.15	0.37
Thrust efficiency	0.16	0.40

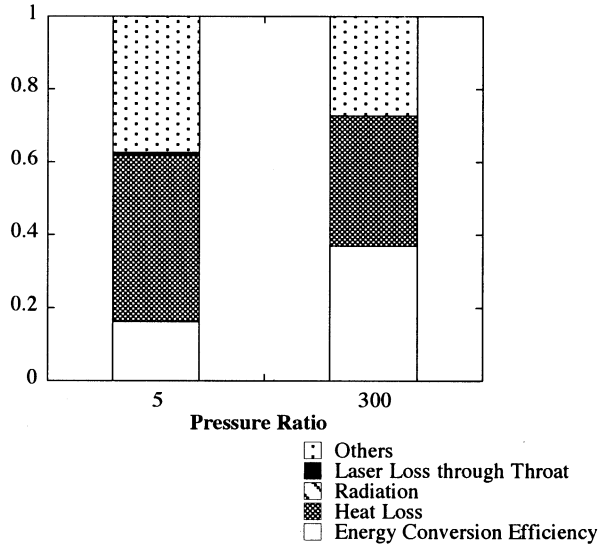

Fig. 15 Energy distribution (700W)

and the temperature difference between inlet and outlet. Figure 12 shows the ratio of the heat loss (fraction of heat loss) to the incident laser power. This heat loss fraction was about 40%.

The laser power passing through the throat was measured using a calorimeter. The ratio of the laser power through the throat to the power without the LSP was defined as the energy loss through the throat. The ratio of this loss to the incident laser power was about 1%.

Figure 13 shows the radiation loss measurement system. The radiation loss through a quartz ring was estimated by measuring both temperature and flow rate of cooling water in a way similar to the heat loss measurement. In the case of P=700W, the measured radiation loss was about 70W. If the plasma is a point, total radiation loss is about 400W. In fact, since the plasma had an elliptical shape, the total radiation was estimated to be less than 400W.

Energy Distribution

To investigate the energy conversion efficiency under high pressure ratio conditions, the air from the nozzle exit was evacuated. The thrust measurement system is shown in Fig. 14. The thruster was connected with a bellows, and the thrust was measured with a load-cell censor. In the measurements, the differences in thrust with and without plasma were measured. The result is shown in Table 1. Here the cold gas thrust under vacuum conditions was calculated by multiplying the value of the thrust under atmospheric condition by Cf (1.5). The efficiency of energy conversion from incident laser power to kinetic energy in the thrust direction was defined as the energy conversion efficiency. It was calculated as,

$$\eta_E = \frac{F^2 - F^2_{cold}}{2\dot{m}P} \qquad (6)$$

where P is the incident laser power and F_{cold} is the thrust of cold gas. In the case of vacuum, the energy conversion efficiency increased up to 37%.

Figure 15 shows the energy distribution. The energy conversion efficiency was about 17%, the heat loss was about 40%, and other losses comprised about 40%.

The heat loss can be recovered to some degree as the propellant enthalpy by means of regenerative cooling. For a pressure ratio of 300, C_F was equal to 1.5 and the thrust increased 1.5 times. The energy conversion

efficiency became 37%, proportional to the square of C_F, namely 2.25 times higher and 20% of the incident power was recovered from other losses as the thrust efficiency.

From this result, it was found that the energy conversion efficiency rose with increase in pressure ratio.

Conclusions

1) An LSP was produced and maintained under low power conditions. It was possible to control the LSP position by means of shifting the focal point of laser beam. Also, it was found that the control of LSP position can enhance the heat transfer from the LSP to the propellant.

2) Thruster performance was evaluated by means of the thrust measurement. The thrust was found to be proportional to the gas pressure. To this respect, it was found that the recovery efficiency of the nozzle contributed much to the thrust efficiency and that it was necessary to increase the pressure ratio.

3) The energy distribution became clear from the measurement of thrust, heat loss and power loss through the nozzle. The energy converted from incident laser power into thrust was about 37%.

Acknowledgments

The authors gratefully acknowledge the financial support provided by Takahashi Industrial and Economic Research Foundation.

References

[1] Birkan M. A. : Laser propulsion. Research status and needs, Journal of Propulsion and Power, Vol. 8, No. 2, 1992, pp. 354-360

[2] Jeng, S. Litchford, R. and Keefer, D. : Comptational Design of an Experimental Laser-Powered Thruster, NASA CR 183587

[3] Zerkle, D. K. Schwartz, S. Mertogul, A. Chen, X. Krier, H. and Mazumder, J. : Laser-Sustained Argon Plasmas for Thermal Rocket Propulsion, Jounal of Propulsion and Power, Vol. 6, No. 1, 1990, pp. 38-45

[4] Black, J. Krier, H. and Glumb, R. J. : Laser Propulsion 10-kW Thruster Test Program Results, Jounal of Propulsion and Power, Vol. 11, No. 6, 1995, pp. 1307-1316

[5] Sutton, G. P. : Rocket Propulsion Elements, John Wiley & Sons.